THE JOURNAL OF PHYSICAL CHEMISTRY A
A JOURNAL OF THE AMERICAN CHEMICAL SOCIETY

pubs.acs.org/JPCA

Article

Mechanistic Studies on the Reaction of $HOClO_2$ with OH Radical on Aqueous Surfaces

Published as part of The Journal of Physical Chemistry A special issue "Joseph S. Francisco Festschrift".

Fei Xu,[#] Jie Zhong,[#] Mohammad Hassan Hadizadeh,[#] Yongxia Hu, Qi Yin, Weina Zhang, Yee Jun Tham, Taicheng An,* Joseph S. Francisco,* and Alfonso Saiz-Lopez*

Cite This: *J. Phys. Chem. A* 2026, 130, 4066−4073

Read Online

ACCESS | Metrics & More | Article Recommendations | Supporting Information

ABSTRACT: Chloric acid ($HOClO_2$) is a newly detected compound in the atmosphere and is involved in ozone depletion. The reaction of $HOClO_2$ with OH radical is likely one of its main atmospheric loss processes. Aqueous surfaces have been reported as critical media for reactions of some chlorine acids, such as HOCl/HCl. However, their effect on the reaction of $HOClO_2$ with OH remains unexplored. Here, we use Born−Oppenheimer molecular dynamics simulations to investigate the reaction of $HOClO_2$ with OH on an aqueous surface. The interfacial behaviors of the reactant ($HOClO_2$) and product (ClO_3) involved in this reaction were investigated. Gas phase $HOClO_2$ can be absorbed on the aqueous surface by forming H-bonds between the acidic H atoms and water. As $HOClO_2$ penetrates the sublayer, it rapidly dissociates into $OClO_2^-$ and H_3O^+; however, before this dissociation, a competitive reaction with OH is likely due to the rapid reactivity of the radical. The reaction of $HOClO_2$ with OH on the aqueous surface follows hydrogen abstraction mechanisms; these include the direct and water monomer/dimer-mediated abstraction pathways. Direct abstraction has no energy barrier and is most kinetically favored, compared to ∼0.5 kcal mol^{-1} and ∼3.0 kcal mol^{-1} for the water monomer- and dimer-mediated mechanisms, respectively. The resulting ClO_3 can reside on the surface with its Cl atom exposed to the air, increasing the potential for further reactions with other atmospheric species. Overall, the specific reaction of $HOClO_2$ with OH on the water surface, could lead to new chlorine recycling by converting $HOClO_2$ into reactive species.

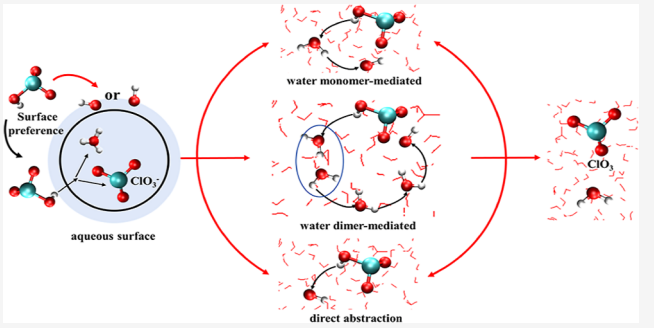

1. INTRODUCTION

Atmospheric ozone (O_3) depletion remains a critical environmental challenge, particularly in polar regions where chlorine cycling drives significant loss[1,2] with implications for climate.[3] While progress has been made in protecting the stratospheric O_3 layer, challenges persist in the lower stratosphere.[4] In the polar environment, reactive chlorine species (Cl, ClO) catalyze O_3 destruction, but their abundance depends critically on the conversion of reservoir species into active forms.[5,6] Heterogeneous reactions on snow, ice, cloud, or aerosol surfaces effectively catalyze these conversions, constituting a primary cause for rapid polar O_3 loss.[5−8]

Chlorine acids are considered key chlorine reservoir substances in the atmospheric chlorine cycling. For example, hypochlorous acid (HOCl), produced from $ClONO_2$ hydration on ice surfaces,[7] undergoes photodissociation to form Cl atom. Moreover, HOCl can react with other chlorine acids, such as hydrochloric acid (HCl), to form Cl_2, which releases Cl atom upon photolysis.[8] While low valence chlorine acids have been widely examined,[9−11] high valence chlorine acids such as chloric acid ($HOClO_2$) and perchloric acid ($HOClO_3$) remain less explored. Jaeglé et al. predicted the existence of $HOClO_3$ in the stratosphere by using box model.[12] Chlorate (ClO_3^-) and perchlorate (ClO_4^-) were identified in stratospheric aerosols, rain, and ice caps,[13−16] suggesting the atmospheric formation of $HOClO_2$ and $HClO_4$. High valence chlorine acids can convert to HOCl, HCl, ClO, ClO_2, and Cl_2 through both gaseous and aqueous reactions.[17−19] All of these products have significant effects on O_3 depletion.[20−22] Thus, high valence chlorine acids are theoretically considered to be possible missing reservoirs for atmospheric chlorine chemistry.[23,24] Recently, Tham et al.[1] detected $HOClO_2$ and $HOClO_3$ during the spring season in the Artic atmosphere. However, a notable absence of high valence chlorine acids contents in atmospheric chlorine chemistry models exists and is largely caused by the

Received: July 6, 2025
Revised: April 7, 2026
Accepted: May 6, 2026
Published: May 13, 2026

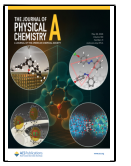

lack of understanding of their fate and removal mechanisms; this leads to inaccurate assessments of the impact of atmospheric chlorine chemistry on O_3 depletion.

In the atmosphere, $HOClO_2$ is mainly removed through deposition on aerosol and snow particles and reactions with various atmospheric oxidants, such as OH, Cl, ClO, and NO_3.[1] The degradation of $HOClO_2$ under photolysis is relatively insignificant.[1] Among these oxidants, OH is commonly recognized to play a central role in determining the atmospheric oxidation capacity. However, the gas-phase reaction of $HOClO_2$ with OH likely has a relatively low rate constant and do not affect the loss of HOClO2.[1] In the polar atmosphere, the low temperature promotes the condensation of water vapor into liquid or solid forms.[5,6] As a result, aqueous surfaces are prevalent in the forms of aerosols, clouds, or sea-salt particles. Specifically, a considerable amount of water molecules also exists in the quasi-liquid layer (QLL) of snow, ice, frost flowers, or snowpack.[5,6] These have been extensively identified as critical media for chlorine reactions, such as the hydration of $ClONO_2$,[25,26] reactions between HOCl and HCl,[8,27] and the photodissociation of HOCl.[28] The reaction mechanisms of atmospheric chlorine species on these surfaces reportedly differ from those in the gas phase or bulk water.[29−32] Specifically, aqueous surfaces are reported to play a much stronger catalytic role in the HClO + OH and HCl + OH reactions by forming complex hydrogen bond networks than water molecules by serving as a "water bridge" in the atmosphere.[9,33−36] Therefore, to better understand the fate of $HOClO_2$ in the polar atmosphere, the detailed reaction mechanisms of $HOClO_2$ with OH on aqueous surfaces need to be examined. However, to date, the reaction potential of $HOClO_2$ with OH on aqueous surfaces and the effect of interfacial water on this reaction remain unclear.

In this work, the reaction mechanism between $HOClO_2$ and OH radical on the aqueous surface was investigated by combining Born−Oppenheimer molecular dynamics (BOMD) simulations, metadynamics methods, and constrained molecular dynamics (CMD) simulations. This reaction potentially proceeds through two possible routes: (i) gas-phase $HClO_3$ interacts with an OH radical adsorbed on the aqueous surface, or (ii) gas-phase OH interacts with an $HClO_3$ molecule adsorbed on the aqueous surface. For route (i), the OH-covered aqueous surfaces have been predicted to be prevalent in the atmosphere.[37] Additionally, our previous studies observed the strong interface preference and stability of OH on aqueous surfaces; these results indicated that the OH radical was readily available to react with the incoming atmospheric $HOClO_2$.[38,39] For route (ii), the solvation behavior of $HOClO_2$ on aqueous surfaces currently remains unknown; thus, the understanding of its interface orientation, stability, and further reaction mechanism is not complete. To better estimate the reaction feasibility of route (ii), particular attention was placed primarily on the interaction of $HOClO_2$ with the aqueous surface. This study begins by examining the solvation behavior and surface preference of $HOClO_2$ on aqueous and ice surfaces using Born−Oppenheimer molecular dynamics (BOMD) simulations and metadynamics (MTD) method. We then explore the detailed reaction mechanisms of $HOClO_2$ with OH radicals, including direct hydrogen abstraction and water-mediated pathways, using constrained molecular dynamics (CMD) method. Finally, we discuss the behavior of the reaction products and their atmospheric implications for chlorine recycling and ozone depletion in polar regions.

2. COMPUTATIONAL METHODS

To investigate the reaction mechanisms of $HClO_3$ with OH radicals on aqueous surfaces, we employed a combination of BOMD simulations, metadynamics, and CMD approaches. The aqueous surface was modeled as a nanodroplet composed of 191 water molecules. This nanodroplet geometry realistically represents curved aqueous interfaces relevant to atmospheric aerosols and clouds, while balancing computational cost. Previous comparisons with planar slab models showed no significant differences in interfacial properties or reaction mechanisms,[40] confirming the robustness of our results to the chosen geometry. This model balances computational cost and accuracy by capturing critical interfacial properties such as hydrogen bonding dynamics, reactivity, and molecular orientation. Periodic boundary conditions were applied in all dimensions to mimic realistic interfacial interactions. BOMD simulations were conducted using the CP2K package,[41] at the BLYP-D3 level. The BLYP D3 functional was chosen for consistency with prior interfacial studies of chlorine containing species.[36,42,43] Meanwhile, benchmark calculations on a related interfacial reaction show good agreement between BLYP-D3 and SCAN-D3,[44] supporting the qualitative reliability of our findings. The Grimme's dispersion correction was used to account for weak intermolecular interactions along with Goedecker−Teter−Hutter (GTH) norm-conserving pseudopotentials. A double-ζ Gaussian basis set combined with an auxiliary plane-wave basis set (energy cutoffs of 280 Ry for plane waves and 40 Ry for Gaussians), and the *NVT* ensemble with a Nose−Hoover chain thermostat to maintain a temperature of 300 K for aqueous surfaces (60 K below the freezing point for the BLYP-D3 functional). The stability of the simulation setup was confirmed through energy conservation tests during BOMD simulations and relaxation of initial configurations using spin-polarized DFT (which showed no significant atomic displacements). For metadynamics, potential walls were placed at $z \approx 1.1$ Å and 18.5 Å to confine the collective variable, and Gaussian hills of height 0.027 eV and width 0.16 Å were added every 50 fs. Meanwhile, the free energy barriers for the three representative pathways (direct, water-monomer-mediated, water-dimer-mediated) were subsequently computed using CMD simulations with a simulation length of 6400 fs and a constraint growth rate of 0.00025 Å/fs to scan R (reaction coordinate). R is defined as the difference between the O−H bond length in $HOClO_2$ and that being formed with the abstracting species (OH or H_2O). This detailed computational approach allows us to accurately capture the interfacial behaviors, reaction mechanisms, and energetic profiles of the $HOClO_2$ + OH system, shedding light on its atmospheric implications (see the Supporting Information for details).

3. RESULTS AND DISCUSSION

3.1. Interactions of $HOClO_2$ with the Aqueous Surfaces

The solvation behaviors, such as the surface preferences, hydrogen bond formations, and molecular orientations of $HOClO_2$ on the aqueous surface are explored using unbiased BOMD simulations (~5 ps) and the metadynamics method (~60 ps). The convergence of the metadynamics simulations was carefully monitored (see Supporting Information, Section S1.2). The four plausible isomers of $HOClO_2$ are labeled A−D in Figure S1. Isomer C ($HOClO_2$) is the most stable form, being lower in Gibbs free energy by 10.5 kcal mol^{-1} relative to isomer A, 27.5 kcal mol^{-1} relative to isomer B, and 36.8 kcal mol^{-1} relative to isomer D, based on gas-phase calculations at the MP2/6−311G(2df,2p) level of theory.[45] Accordingly, a detailed investigation of the solvation behavior of isomer C of $HOClO_2$ is presented in the following section. Similar to the behavior of HOCl,[42] $HOClO_2$ also can be easily adsorbed on the aqueous interface from the gas phase. Here, the "water

https://doi.org/10.1021/acs.jpca.5c04670
J. Phys. Chem. A 2026, 130, 4066−4073

surface" is defined as the Gibbs dividing surface—the radial position where the water density drops to 50% of the bulk density (see Figure S2 in Supporting Information).

$HOClO_2$ readily dissolves in water and its acidic properties are well-known. However, the molecular mechanism of its interaction with atmospheric aqueous surfaces (modeled here as nanodroplets) remains elusive. Here, we study the free energy profile of $HOClO_2$ as it transitions from the gas phase to interior region of aqueous (Figure 1A), using the

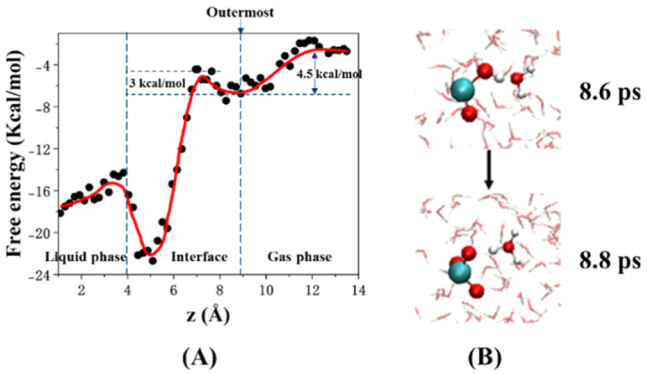

Figure 1. (A) Free energy profile of $HOClO_2$ migrating from the gas phase to the bulk. The red line represents the fit to the scatter by the least-squares fitting method. The free energy profile highlights the distinct regions: z = 14 to 9 Å (interface, energy release of ∼4.5 kcal mol^{-1}), and z = 9 to 7 Å (one water layer, energy barrier of ∼3.0 kcal mol^{-1}). Where z < 7 Å indicates the free energy profile of $OClO_2^-$ ion migrating from water surface to interior region of aqueous. (B) Dissociation of $HOClO_2$.

metadynamics method with an ∼60 ps BOMD simulation. In these metadynamics simulations, the distance between the $HOClO_2$ molecule and the center of mass of the water droplet along the direction perpendicular to the air−water interface (z-coordinate) was used as the collective variable (CV). As shown in Figure 1A, the adsorption of gaseous $HOClO_2$ on the water surface releases 4.5 kcal mol^{-1} of free energy, which indicates the strong preference of $HOClO_2$ for aqueous surfaces. This is consistent with the observations reported by Tham et al., who proposed that $HOClO_2$ is removed through heterogeneous uptake on aerosol and snow surfaces, providing a sink for reactive Cl in the Arctic boundary.[1] Meanwhile, $HOClO_2$ continues to migrate from the water surface to a depth of one water layer via a ∼3 kcal mol^{-1} free energy barrier. After entering the sublayer of the surface, it readily dissociates to $OClO_2^-$ and $H3O^+$ nearly instantaneously within the simulation time scale (Figure 1B). In agreement with previous studies, $HOClO_2$ can be easily ionized into ClO_3^- because of its high acidity.[1] Finally, the $OClO_2^-$ ions continue migrating into the bulk region by overcoming a certain free energy, followed by a plateau. The above results indicate that $HOClO_2$ tends to present both molecular and ion forms at the water surface in, and present mainly ion form in the bulk aqueous phase.

Next, the interaction of $HOClO_2$ with interfacial water was investigated. Figure S3 shows the radial distribution function (RDF) profiles between $HOClO_2$ and water on the aqueous surface, obtained from unbiased BOMD trajectories, where the H-bond has a large chance to break, as shown in Figures S4 and S5 (see the Supporting Information for further details). The four $HOClO_2$−water complexes are characterized by distinct hydrogen-bonding interactions involving the H atom or O atoms of $HOClO_2$ with neighboring water molecules. These complexes include configurations where $HOClO_2$ forms one or more hydrogen bonds with interfacial water, as shown in Figure S6 of the Supporting Information. A dominant complex (Complex 1) involves hydrogen bonding through the H atom of $HOClO_2$, with a probability of 57.5% on the aqueous surface.

Moreover, the orientation of the atmospheric species on the water surface affects the probability of collisions between reactants and the magnitude of the reaction potential barriers.[24,46] Herein, the orientation of $HOClO_2$ is investigated by the distribution of angle θ calculated from the same unbiased BOMD simulations; this angle is formed by two vectors: (i) the vector perpendicular to the water surface and (ii) the vector from O1 to the Cl atom of $HOClO_2$. As shown in Figure 2A, θ is mostly distributed within 90° on the aqueous

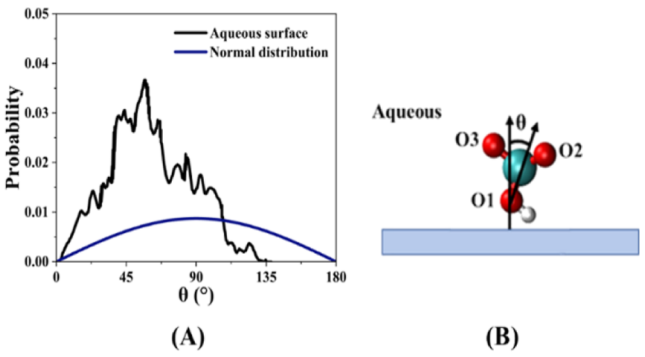

Figure 2. (A,B) θ distributions for $HOClO_2$ on aqueous surfaces. The blue curve represents the regular distribution 1/2 sin(θ).

surface, which is similar to that of HOCl.[42] Where, the entire group of ClO_2 is exposed on the outside of the aqueous surface. A comparison of the solvation behaviors of $HOClO_2$ and the OH radical on water surfaces revealed important differences. OH radicals exhibit strong surface preferences on both the outer and sublayers of a droplet and can exist stably at these locations,[38,39] whereas $HOClO_2$ rapidly dissociates into $OClO_2^-$ and H_3O^+ upon reaching the sublayer.

The OH radical has higher reactivity than $HOClO_2$ because of its unpaired electron, smaller size, and higher mobility; these attributes enable easier collisions and interactions. Additionally, our previous work has demonstrated that OH radicals can remain stably adsorbed at water interface for extended time scales (exceeding 100 ps),[38,39] which is much longer than the dissociation time of $HOClO_2$ within 8.8 ps after interacting with the aqueous sublayer. Consequently, OH can reach and accommodate on the surface more readily because of these properties. Hence, route (i) favors over route (ii); in route (i), gas-phase $HOClO_2$ reacts with the preadsorbed OH radical on the aqueous surface, and in route (ii), gas-phase OH reacts with the preadsorbed $HOClO_2$. Therefore, in the following section on the mechanism of the reaction of $HOClO_2$ with OH, reaction route (i) is further examined.

3.2. Reaction of $HOClO_2$ with OH on the Aqueous Surface

To investigate this reaction further, the reaction mechanisms of $HOClO_2$ with OH on the aqueous surface are conducted using BOMD simulations coupled with CMD simulations; moreover, the reaction trajectory, energy barrier, and the surface preferences of the remaining products are also examined.

https://doi.org/10.1021/acs.jpca.5c04670
J. Phys. Chem. A 2026, 130, 4066−4073

Our previous studies on the solvation process of the OH radical in water droplets revealed that the OH radical was either vertically located in the outer layer of the water droplet.[38,39] Eight initial $HOClO_2$−OH configurations (S-I to S-VIII) were generated by systematically varying the relative orientations and distances between $HOClO_2$ and OH on the aqueous surface: S-I has OH group of $HOClO_2$ pointing toward OH radical (OH oriented to the surface); S-II is similar S-I but OH perpendicular to the surface from H side; S-III has the acidic hydrogen pointing directly toward OH (hydrogen pointing toward the acidic hydrogen); S-IV has the acidic hydrogen pointing toward OH and OH oriented to the surface; S-V has $HOClO_2$ pointing toward OH and OH oriented to the surface; S-VI has Cl atom of the $HOClO_2$ pointing toward OH and OH oriented perpendicular to the surface; S-VII has the OH group of $HOClO_2$ pointing toward OH and OH oriented perpendicular to the surface; and S-VIII has the acidic hydrogen pointing directly toward OH (OH oriented to the surface). The initial positions and orientations for all systems are shown in Figure S7. Each BOMD simulation for these configurations was run up to 30 ps, sufficient to observe the hydrogen abstraction event. The time evolution of the critical bond formation along with the chemical mechanism related to the reactions of $HOClO_2$ and the OH radical are presented in Figures 3 and S8 and S9 of the Supporting Information. All eight systems exhibit hydrogen atom abstraction mechanisms for the reaction of $HOClO_2$ with OH on the aqueous surface.

Among them, systems I, V, VI, and VIII follow a similar water monomer-mediated pathway: the acidic H atom from $HOClO_2$ first transfers to a mediating water molecule, followed by a second H-transfer to the OH radical, ultimately yielding a new water molecule. This sequential two-step mechanism involves multiple hydrogen transfer events through the mediating water molecule. Systems II and VI are similar, where two water molecules function together to abstract the hydrogen on $HOClO_2$, followed by hydrogen transfer processes with the involvement of water monomers, and finally connect with the OH radical (water dimer-mediated pathway). Systems III and VII are similar; here, hydrogen is directly abstracted from $HOClO_2$ to the OH radical, without the introduction of water molecules (direct abstraction pathway). $OClO_2$ species can be produced on the aqueous surface from these three mechanisms. To comprehensively explore these systems, three representative systems, S-I, S-II, and S-III, which capture the essential features of the three reaction mechanisms in Figure 3, are chosen for further energy calculations in Figure 4. In Figure 4, The direct abstraction and water-monomer-mediated pathways have free energy barriers of 0.0 ± 0.2 kcal mol^{-1} and 0.5 ± 0.3 kcal mol^{-1}, respectively, which are lower than the barrier for the water-dimer-mediated pathway (3.0 ± 0.4 kcal mol^{-1}), indicating that the former two pathways are kinetically more favorable under the studied conditions. Where, the reaction coordinate R is defined as the difference between the O−H bond distance in $HOClO_2$ and the O−H bond distance being formed with the abstracting species (OH or water). Additionally, a previous study reported that the HCl + OH reaction also occurred mainly through the direct hydrogen abstraction mechanism on droplet surfaces;[34] in agreement with our observations of the $HOClO_2$ + OH reaction.

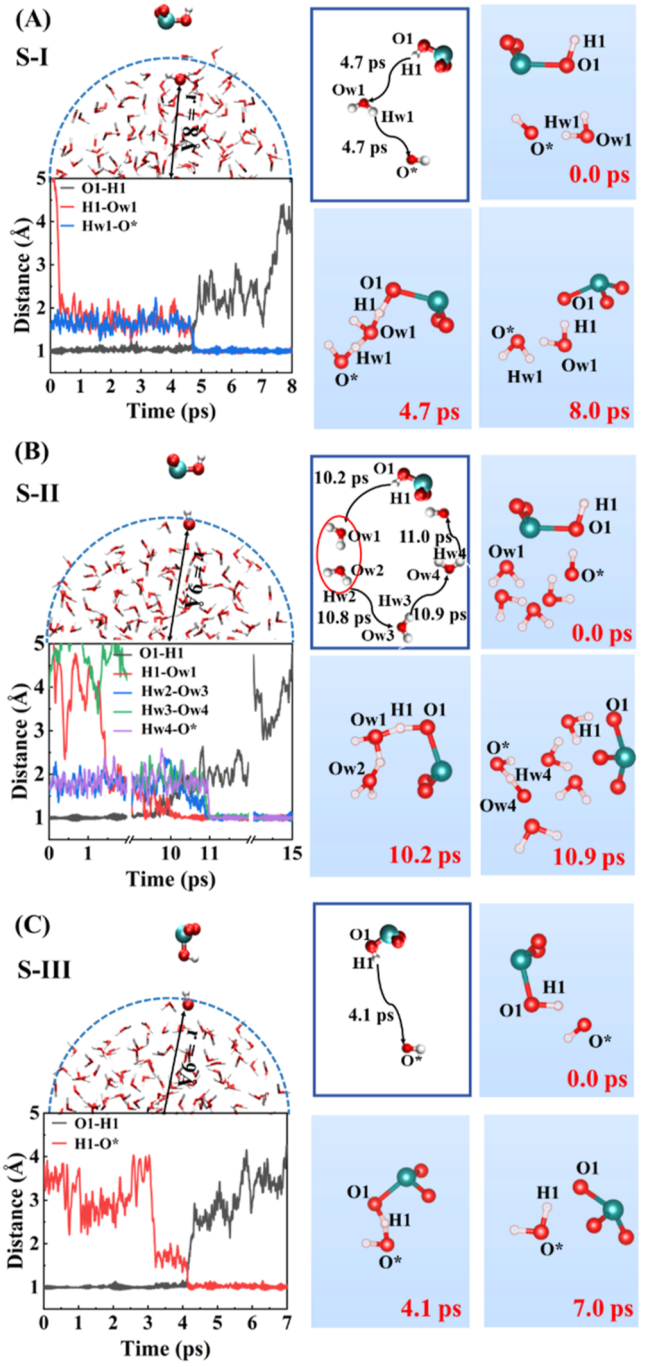

Figure 3. Time evolution of critical bond formation from AIMD trajectories for (A) S-I, (B) S-II, and (C) S-III systems, showing hydrogen abstraction by water monomers, dimers, and direct abstraction, respectively. Graphs display bond distances over time for key bond-breaking and forming events during the reaction between $HOClO_2$ and OH on the aqueous surface. Corresponding snapshots and schematics highlight intermediates and pathways, illustrating critical bond changes and reaction mechanisms.

3.3. Interactions of $OClO_2$ with the Aqueous Surfaces

To gain deeper insight into the hydrogen abstraction mechanisms of $HOClO_2$, we investigated the behavior of the resulting $OClO_2$ species on the aqueous surface using unbiased BOMD simulations. Figure S10 depicts the RDF profiles between $OClO_2$ and surrounding water molecules. Hydrogen bonds are defined using geometric criteria: donor−acceptor

https://doi.org/10.1021/acs.jpca.5c04670
J. Phys. Chem. A 2026, 130, 4066−4073

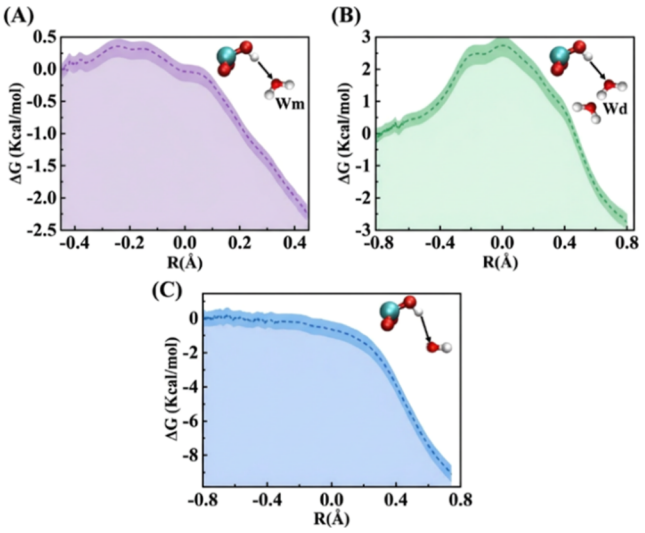

Figure 4. (A–C) Free energy barriers of the acidic hydrogen abstraction of $HOClO_2$ by OH via the water monomer-mediated, water dimer-mediated, and direct pathways related to systems S-I, S-II, and S-III, respectively. The error bars represent one standard deviation calculated from three independent CMD simulations for each pathway (see Supporting Information, Section S1.3).

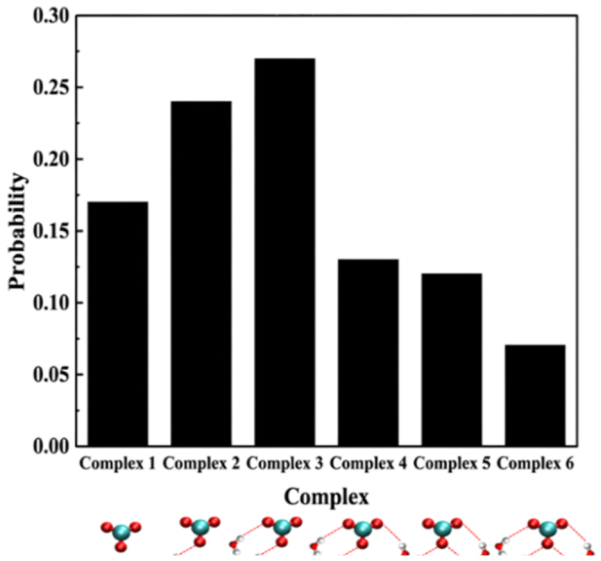

Figure 5. Probabilities of the different complexes forming between $OClO_2$ and interfacial water on aqueous surfaces. The hydrogen bonding patterns illustrated are schematic representations.

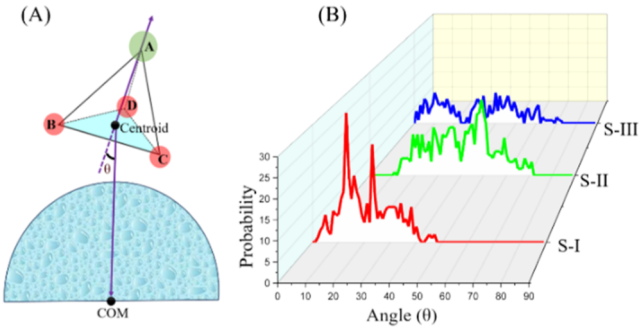

Figure 6. (A,B) θ distributions of $OClO_2$ on aqueous surfaces related to typical S-I, S-II, and S-III systems.

distance <3.5 Å and D–H···A angle ≥150°. The RDF profiles show that all three oxygen atoms of $OClO_2$ exhibit similar interaction patterns to $H–O(H_2O)$, with an evident peak located at ∼1.9 Å. These peaks indicate that $OClO_2$ has a high probability of forming hydrogen bonds through all of its O atoms with neighboring water molecules. This result is different from the phenomenon of $HOClO_2$ on the aqueous surface above (Figure S3), in which $HOClO_2$ shows a clear preference for hydrogen bonding, mainly through its H atom, with less involvement of its O atoms. Additionally, the similarity in the peak positions and intensities for all three $H–O(H_2O)$ bonds indicates that all three O atoms have comparable hydrogen bonding capabilities on the aqueous surface. Similar to $HOClO_2$, no evident interaction is found between Cl and $O(H_2O)$ for $OClO_2$ on the aqueous surfaces.

The probabilities of the five typical complexes formed between $OClO_2$ and the interfacial water on aqueous surfaces are shown in Figure 5. Similar to the structure of $HOClO_2$, the interaction of $OClO_2$ with the aqueous surface is attributed mainly to the H-bonds from the O atom of $OClO_2$ with surrounding H atoms. As shown in Figure 5, in Complex 2 and Complex 3, $OClO_2$ forms one or two H-bonds with the neighboring water molecules; here, these complexes are dominant on the aqueous surface, with probabilities of 24.4% and 26.7%, respectively. In Complex 1, $OClO_2$ provides no H-bonds; this complex has a probability of 16.3%. In Complex 4 (13.1%), Complex 5 (12.1%) and Complex 6 (7.4%), $OClO_2$ forms three or four hydrogen bonds; these complexes occur with lower probabilities. These results indicate that after hydrogen abstraction, $OClO_2$ tends to form one or two hydrogen bonds with the interfacial water molecules, maintaining some flexibility in its hydrogen bonding behavior.

Next, the preferred orientation of the resulting $OClO_2$ species on the aqueous surface is shown in Figure 6. The atoms of $OClO_2$ adopt a trigonal pyramidal arrangement, with the Cl atom at the apex and the three oxygen atoms forming a triangular base. The orientation of $OClO_2$ is examined by an angle contribution, θ. θ is formed between two vectors: (i) the vector connecting the chlorine atom to the centroid of the triangular oxygen base and (ii) the vector extending from the centroid of the triangle to the center of mass of the water droplet. In Figure 6, we plot the probability of $OClO_2$ on the aqueous surface versus the angle θ for systems S-I, S-II, and S-III. θ is mostly distributed at approximately 10° in system S-I, approximately 40° in system S-II, and between 10° and 40° in system S-III; these results indicate that the triangular oxygen base tends to be parallel to the water surface in all systems, exposing the Cl atom to the outside of the aqueous surface. This is likely attributed to the stronger H-bond formation between $O(OClO_2)$ and $H(H_2O)$ than between $Cl(OClO_2)$ and $H(H_2O)$. As a result, the chlorine atom of $OClO_2$ becomes more accessible for further reactions with trace atmospheric gases.

3.4. Atmospheric Implications of $HOClO_2$ for the Chlorine Chemical Cycle

Our proposed OH-initiated reactions of $HOClO_2$ on the polar water surfaces serve as a potential removal pathway for $HOClO_2$ and have implications for its atmospheric fate. The formed $OClO_2$ is retained on the surface, which can undergo O abstraction by NO, resulting in the formation of NO_2 and ClO_2; here, ClO_2 could further react with NO and finally transfer into ClO and Cl. Consequently, the special OH-

https://doi.org/10.1021/acs.jpca.5c04670
J. Phys. Chem. A 2026, 130, 4066–4073

initiated reactions of $HOClO_2$ on the water surfaces can reactivate chlorine from high valence chlorine acids sources, which potentially constitutes a new active chlorine reservoir in the polar region. However, to comprehensively evaluate their atmospheric fate, the subsequent reactions of ClO_3, as well as the possible reaction pathways of $HOClO_2$ with the typical halogen radicals and halogen ions on aqueous surfaces, need for detailed investigation in future studies.

4. CONCLUSIONS

Based on our investigation, gas phase $HOClO_2$ can be absorbed on the aqueous surface, releasing approximately 4.5 kcal mol^{-1} of free energy as it transitions from the gas phase to the interfacial region. Upon penetrating to a depth of one water layer, overcoming an energy barrier of ∼3.0 kcal mol^{-1}, $HOClO_2$ dissociates into $OClO_2^-$ and H_3O^+ ps. On the aqueous surface, the H-bond network of $HOClO_2$ is similar to that of HOCl and is dominated by the H-bonds formed between the H atoms of acid and water. In addition, the reaction of $HOClO_2$ with OH on the polar water surface follows hydrogen abstraction mechanisms, including direct abstraction, water monomer-mediated abstraction, and water dimer-mediated abstraction pathways. Direct abstraction proceeds without an energy barrier, making it energetically more favorable compared to the water monomer-mediated and water dimer-mediated pathways, which have energy barriers of ∼0.5 kcal mol^{-1} and ∼3.0 kcal mol^{-1}, respectively. These results indicate that the direct abstraction pathway is energetically most favored. Moreover, after hydrogen abstraction from $HOClO_2$, the resulting $OClO_2$ species resides on the surface by forming H-bonds through all of its O atoms with water and orients itself with the Cl atom exposed to the air. Overall, the molecular insights from this study highlight the importance of the aqueous surface on the fate of higher chlorine acids in the chlorine chemical cycle. Importantly, the specific reaction of $HOClO_2$ on the water surface could initiate new chlorine recycling by converting high valence chlorine acids sources into reactive species such as ClO and Cl; these species directly contribute to O_3 depletion. We note that this work is based on calculations at the BLYP-D3 level; the choice of functional can significantly affect the computed energy barriers, and future studies using more accurate methods are warranted for further investigation. Additionally, while this study highlights the fundamental reactivity of $HOClO_2$ with OH on pure water surfaces, the inclusion of salts and surface-active organic species, as present in atmospheric aerosols, could modify interfacial dynamics and reaction pathways. Future work exploring such heterogeneous systems will be critical for refining our understanding of $HOClO_2$ chemistry under more realistic environmental conditions.

■ ASSOCIATED CONTENT

Supporting Information

The Supporting Information is available free of charge at https://pubs.acs.org/doi/10.1021/acs.jpca.5c04670.

Details of the methodological section, minimum-energy structures, density profile, free energy profile, RDF profiles, H-Bonds breaking on the aqueous interface, MSD profiles, initial positions of $HOClO_2$ and the OH radicals, time evolution, and possible reaction mechanism (PDF)

■ AUTHOR INFORMATION

Corresponding Authors

Taicheng An − *Guangdong Key Laboratory of Environmental Catalysis and Health Risk Control, Guangzhou Key Laboratory of Environmental Catalysis and Pollution Control, School of Environmental Science and Engineering, Institute of Environ-mental Health and Pollution Control, Guangdong University of Technology, Guangzhou 510006, China*; orcid.org/0000-0001-6918-8070; Email: antc99@gdut.edu.cn

Joseph S. Francisco − *Department of Earth and Environmental Sciences, University of Pennsylvania, Philadelphia, Pennsylvania 19104, United States*; orcid.org/0000-0002-5461-1486; Email: frjoseph@sas.upenn.edu

Alfonso Saiz-Lopez − *Department of Atmospheric Chemistry and Climate, Institute of Physical Chemistry Blas Cabrera, CSIC, Madrid 28006, Spain*; orcid.org/0000-0002-0060-1581; Email: a.saiz@csic.es

Authors

Fei Xu − *Department of Atmospheric Chemistry and Climate, Institute of Physical Chemistry Blas Cabrera, CSIC, Madrid 28006, Spain; Environment Research Institute, Shandong University, Qingdao 266237, China*

Jie Zhong − *School of Petroleum Engineering, China University of Petroleum (East China), Qingdao 266580, China*; orcid.org/0000-0003-4070-9383

Mohammad Hassan Hadizadeh − *Environment Research Institute, Shandong University, Qingdao 266237, China*

Yongxia Hu − *Environment Research Institute, Shandong University, Qingdao 266237, China*

Qi Yin − *School of Materials Science and Engineering, China University of Petroleum (East China), Qingdao 266580, China*

Weina Zhang − *Guangdong Key Laboratory of Environmental Catalysis and Health Risk Control, Guangzhou Key Laboratory of Environmental Catalysis and Pollution Control, School of Environmental Science and Engineering, Institute of Environ-mental Health and Pollution Control, Guangdong University of Technology, Guangzhou 510006, China*

Yee Jun Tham − *School of Marine Sciences, Sun Yat-sen University, Zhuhai 519082, China*; orcid.org/0000-0001-7924-5841

Complete contact information is available at: https://pubs.acs.org/10.1021/acs.jpca.5c04670

Author Contributions

#F.X., J.Z., and M.H.H. contributed equally to this work. All authors have given approval to the final version of the manuscript.

Notes

The authors declare no competing financial interest.

■ ACKNOWLEDGMENTS

J.S.F. would like to thank the UNL Holland Computing Center for computational support. F.X. is supported by the National Natural Science Foundation of China (No. 22476111, No. 22076103, No. 22236004) and Basic and Applied Basic Research Foundation of Guangdong Province (No.

2023A1515012043). J.Z. is grateful for the support from the DEEDS project and the support from Purdue ITAP for computing resources. M.H.H. is supported by the National Natural Science Foundation of China (No. 42350410435). W.Z. is supported by the National Natural Science Foundation of China (No. 41425015, No. 41907184, No. 41675122).

REFERENCES

(1) Tham, Y. J.; Sarnela, N.; Iyer, S.; Li, Q. Y.; Angot, H.; Quéléver, L. L. J.; Beck, I.; Laurila, T.; Beck, L. J.; Boyer, M.; Carmona-García, J.; Borrego-Sánchez, A.; Roca-Sanjuán, D.; Peräkylä, O.; Thakur, R. C.; He, X. C.; Zha, Q. Z.; Howard, D.; Blomquist, B.; Archer, S. D.; Bariteau, L.; Posman, K.; Hueber, J.; Helmig, D.; Jacobi, H. W.; Junninen, H.; Kulmala, M.; Mahajan, A. S.; Massling, A.; Skov, H.; Sipilä, M.; Francisco, J. S.; Schmale, J.; Jokinen, T.; Saiz-Lopez, A. Widespread detection of chlorine oxyacids in the Arctic atmosphere. *Nat. Commun.* **2023**, *14* (1), 1769.

(2) Solomon, S. Stratospheric ozone depletion: A review of concepts and history. *Rev. Geophys.* **1999**, *37* (3), 275−316.

(3) Saiz-Lopez, A.; Fernandez, R. P.; Li, Q.; Cuevas, C. A.; Fu, X.; Kinnison, D. E.; Tilmes, S.; Mahajan, A. S.; Gómez Martín, J. C.; Iglesias-Suarez, F.; Hossaini, R.; Plane, J. M. C.; Myhre, G.; Lamarque, J. F. Natural short-lived halogens exert an indirect cooling effect on climate. *Nature* **2023**, *618* (7967), 967−973.

(4) Chipperfield, M. P.; Bekki, S.; Dhomse, S.; Harris, N. R.; Hassler, B.; Hossaini, R.; Steinbrecht, W.; Thiéblemont, R.; Weber, M. Detecting recovery of the stratospheric ozone layer. *Nature* **2017**, *549* (7671), 211−218.

(5) Simpson, W. R.; Von Glasow, R.; Riedel, K.; Anderson, P.; Ariya, P.; Bottenheim, J.; Burrows, J.; Carpenter, L. J.; Frieß, U.; Goodsite, M. E.; Heard, D.; et al. Halogens and their role in polar boundary-layer ozone depletion. *Atmos. Chem. Phys.* **2007**, *7* (16), 4375−4418.

(6) Hegglin, M. I.; Fahey, D. W.; McFarland, M.; Montzka, S. A.; Nash, E. R. *Scientific Assessment of Ozone Depletion: 2014—Twenty Questions and Answers About the Ozone Layer: 2014 Update*; World Meteorological Organization, 2015.

(7) Molina, M. J.; Tso, T. L.; Molina, L. T.; Wang, F. C. Y. Antarctic stratospheric chemistry of chlorine nitrate, hydrogen chloride, and ice: Release of active chlorine. *Science* **1987**, *238* (4831), 1253−1257.

(8) Abbatt, J.; Molina, M. J. The heterogeneous reaction of HOCl + HCl → Cl_2 + H_2O on ice and nitric acid trihydrate: Reaction probabilities and stratospheric implications. *Geophys. Res. Lett.* **1992**, *19* (5), 461−464.

(9) Tolbert, M. A.; Rossi, M. J.; Malhotra, R.; Golden, D. M. Reaction of chlorine nitrate with hydrogen chloride and water at Antarctic stratospheric temperatures. *Science* **1987**, *238* (4831), 1258−1260.

(10) Casassa, S.; Pisani, C. Interaction of HOCl with a chlorinated ice surface to produce molecular chlorine: An ab-initio study. *J. Chem. Phys.* **2002**, *116* (22), 9856−9864.

(11) Gonzalez, J.; Anglada, J. M.; Buszek, R. J.; Francisco, J. S. Impact of water on the OH + HOCl reaction. *J. Am. Chem. Soc.* **2011**, *133* (10), 3345−3353.

(12) Jaeglé, L.; Yung, Y. L.; Toon, G. C.; Sen, B.; Blavier, J. F. Balloon observations of organic and inorganic chlorine in the stratosphere: The role of $HClO_4$ production on sulfate aerosols. *Geophys. Res. Lett.* **1996**, *23* (14), 1749−1752.

(13) Furdui, V. I.; Zheng, J.; Furdui, A. Anthropogenic perchlorate increases since 1980 in the Canadian High Arctic. *Environ. Sci. Technol.* **2018**, *52* (3), 972−981.

(14) Murphy, D. M.; Thomson, D. S. Halogen ions and NO^+ in the mass spectra of aerosols in the upper troposphere and lower stratosphere. *Geophys. Res. Lett.* **2000**, *27* (19), 3217−3220.

(15) Dasgupta, P. K.; Martinelango, P. K.; Jackson, W. A.; Anderson, T. A.; Tian, K.; Tock, R. W.; Rajagopalan, S. The origin of naturally occurring perchlorate: The role of atmospheric processes. *Environ. Sci. Technol.* **2005**, *39* (6), 1569−1575.

(16) Furdui, V. I.; Tomassini, F. Trends and sources of perchlorate in Arctic snow. *Environ. Sci. Technol.* **2010**, *44* (2), 588−592.

(17) Zhu, R. S.; Lin, M. C. An ab initio chemical kinetic study on the reactions of H, OH, and Cl with $HOClO_3$. *Int. J. Chem. Kinet.* **2010**, *42* (4), 253−261.

(18) Yin, G.; Ni, Y. Mechanism of the ClO_2 generation from the H_2O_2-HOClO2 reaction. *Can. J. Chem. Eng.* **2000**, *78* (4), 827−833.

(19) Monteiro, M. K. S.; Monteiro, M. M. S.; de Melo Henrique, A. M.; Llanos, J.; Saez, C.; Dos Santos, E. V.; Rodrigo, M. A. A review on the electrochemical production of chlorine dioxide from chlorates and hydrogen peroxide. *Curr. Opin. Electrochem.* **2021**, *27*, 100685.

(20) Solomon, S.; Stone, K.; Yu, P.; Murphy, D. M.; Kinnison, D.; Ravishankara, A. R.; Wang, P. Chlorine activation and enhanced ozone depletion induced by wildfire aerosol. *Nature* **2023**, *615* (7951), 259−264.

(21) Cicerone, R. J.; Walters, S.; Stolarski, R. S. Chlorine compounds and stratospheric ozone. *Science* **1975**, *188* (4186), 378−379.

(22) Anderson, J. G.; Weisenstein, D. K.; Bowman, K. P.; Homeyer, C. R.; Smith, J. B.; Wilmouth, D. M.; Sayres, D. S.; Klobas, J. E.; Leroy, S. S.; Dykema, J. A.; Wofsy, S. C. Stratospheric ozone over the United States in summer linked to observations of convection and temperature via chlorine and bromine catalysis. *Proc. Natl. Acad. Sci. U. S. A.* **2017**, *114* (25), 4905−4913.

(23) Sander, S. P.; Friedl, R. R.; Yung, Y. L. Rate of formation of the ClO dimer in the polar stratosphere: Implications for ozone loss. *Science* **1989**, *245* (4922), 1095−1098.

(24) Alkoby, Y.; Chadwick, H.; Godsi, O.; Labiad, H.; Bergin, M.; Cantin, J. T.; Litvin, I.; Maniv, T.; Alexandrowicz, G. Setting benchmarks for modelling gas-surface interactions using coherent control of rotational orientation states. *Nat. Commun.* **2020**, *11* (1), 3110.

(25) McNamara, J. P.; Hillier, I. H. Exploration of the mechanism of the hydrolysis of chlorine nitrate in small water clusters using electronic structure methods. *J. Phys. Chem. A* **1999**, *103* (36), 7310−7321.

(26) Xu, S. C.; Zhao, X. S. Theoretical investigation of the reaction of $ClONO_2$ with H_2O on water clusters. *J. Phys. Chem. A* **1999**, *103* (13), 2100−2106.

(27) Voegele, A. F.; Tautermann, C. S.; Loerting, T.; Liedl, K. R. Reactions of HOCl + HCl + nH_2O and HOCl + HBr + nH_2O. *J. Phys. Chem. A* **2002**, *106* (34), 7850−7857.

(28) Minaev, B. F. The singlet-triplet absorption and photo-dissociation of the HOCl, HOBr, and HOI molecules calculated by the MCSCF quadratic response method. *J. Phys. Chem. A* **1999**, *103* (36), 7294−7309.

(29) Du, S.; Francisco, J. S.; Schenter, G. K.; Garrett, B. C. Interaction of ClO radical with liquid water. *J. Am. Chem. Soc.* **2009**, *131* (41), 14778−14785.

(30) Zhong, J.; Zhu, C.; Li, L.; Richmond, G. L.; Francisco, J. S.; Zeng, X. C. Interaction of SO_2 with the surface of a water nanodroplet. *J. Am. Chem. Soc.* **2017**, *139* (47), 17168−17174.

(31) Zhong, J.; Kumar, M.; Zhu, C. Q.; Francisco, J. S.; Zeng, X. C. Surprising stability of larger Criegee intermediates on aqueous interfaces. *Angew. Chem., Int. Ed.* **2017**, *56* (27), 7740−7744.

(32) Zhong, J.; Wang, C.; Zeng, X. C.; Francisco, J. S. Heterogeneous reactions of SO_3 on ice: An overlooked sink for SO_3 depletion. *J. Am. Chem. Soc.* **2020**, *142* (5), 2150−2154.

(33) Buszek, R. J.; Barker, J. R.; Francisco, J. S. Water effect on the OH+ HCl reaction. *J. Phys. Chem. A* **2012**, *116* (19), 4712−4719.

(34) Mallick, S.; Kumar, P. OH + HCl reaction at the surface of a water droplet: An ab initio molecular dynamical study. *J. Phys. Chem. B* **2020**, *124* (12), 2465−2472.

(35) Kumar, M.; Francisco, J. S. Elucidating the molecular mechanisms of Criegee-amine chemistry in the gas phase and aqueous surface environments. *Chem. Sci.* **2019**, *10* (3), 743−751.

(36) Wan, Z.; Zhu, C.; Francisco, J. S. Molecular insights into the spontaneous generation of Cl_2O in the reaction of $ClONO_2$ and

https://doi.org/10.1021/acs.jpca.5c04670
J. Phys. Chem. A 2026, 130, 4066−4073

HOCl at the air-water interface. *J. Am. Chem. Soc.* **2023**, *145* (31), 17478−17484.
(37) Vácha, R.; Slavíček, P.; Mucha, M.; Finlayson-Pitts, B. J.; Jungwirth, P. Adsorption of atmospherically relevant gases at the air/water interface: Free energy profiles of aqueous solvation of N_2, O_2, O_3, OH, H_2O, HO_2, and H_2O_2. *J. Phys. Chem. A* **2004**, *108* (52), 11573−11579.
(38) Hadizadeh, M. H.; Pan, Z.; Azamat, J. Investigation of OH radical in the water nanodroplet during vapor freezing process: An ab initio molecular dynamics study. *J. Mol. Liq.* **2021**, *343*, 117597−117609.
(39) Hadizadeh, M. H.; Yang, L.; Fang, G.; Qiu, Z.; Li, Z. The mobility and solvation structure of a hydroxyl radical in a water nanodroplet: A Born-Oppenheimer molecular dynamics study. *Phys. Chem. Chem. Phys.* **2021**, *23* (27), 14628−14635.
(40) Chen, S.; Zhu, J.; Li, J.; Guo, P.; Yang, J.; He, X. Entropy-driven difference in interfacial water reactivity between slab and nanodroplet. *Nat. Commun.* **2025**, *16* (1), 5250.
(41) VandeVondele, J.; Krack, M.; Mohamed, F.; Parrinello, M.; Chassaing, T.; Hutter, J. Quickstep: Fast and accurate density functional calculations using a mixed Gaussian and plane waves approach. *Comput. Phys. Commun.* **2005**, *167* (2), 103−128.
(42) Zhong, J.; Zhang, W.; Wu, S.; An, T.; Francisco, J. S. Molecular interaction and orientation of hocl on aqueous and ice surfaces. *J. Am. Chem. Soc.* **2020**, *142* (41), 17329−17333.
(43) Zhang, W.; Zheng, D.; Han, H.; Wan, Z.; Zhong, J.; Ji, Y.; Li, G.; Francisco, J. S.; An, T. Promoting Cl2O generation from the HOCl+ HOCl reaction on aqueous/frozen air−water interfaces. *J. Am. Chem. Soc.* **2024**, *146* (46), 31935−31944.
(44) Zeng, F.; Yu, X.; Li, X.; Xie, H.-B.; Chen, J.; Xia, D.; Francisco, J. S. Molecular insights into the spontaneous generation of CO2 in reaction of CO and HOCl at air−water interfaces. *J. Am. Chem. Soc.* **2025**, *147* (43), 39701−39707.
(45) Francisco, J. S.; Sander, S. P. Structures, relative stabilities, and vibrational spectra of isomers of HOClO2. *J. Phys. Chem.* **1996**, *100* (2), 573−579.
(46) Hoffmann, D. K.; Paintner, T.; Limmer, W.; Petrov, D. S.; Denschlag, J. H. Reaction kinetics of ultracold molecule-molecule collisions. *Nat. Commun.* **2018**, *9* (1), 5244.

https://doi.org/10.1021/acs.jpca.5c04670
J. Phys. Chem. A 2026, 130, 4066−4073